

ESI

**Fe<sub>3</sub>O<sub>4</sub> nanoparticles decorated on CuS platelets based sphere: A popcorn chicken-like heterostructure as an ideal material against electromagnetic pollution**

Xiaodong Sun,<sup>a</sup> Mingxu Sui,<sup>a</sup> Guangzhen Cui,<sup>a</sup> Ling Li,<sup>a</sup> Xiaopeng Li,<sup>c</sup> Xuliang Lv,<sup>\*a</sup> Fan Wu<sup>\*b</sup> and Guangxin Gu<sup>\*d</sup>

*a. Key Laboratory of Science and Technology on Electromagnetic Environmental Effects and Electro-optical Engineering, The Army Engineering University of PLA, Nanjing, 210007, P. R. China. E-mail: [xllu1957@126.com](mailto:xllu1957@126.com) (X. Lv)*

*b. School of Mechanical Engineering, Nanjing University of Science and Technology, Nanjing 210094, P. R. China. E-mail: [wufan@njust.edu.cn](mailto:wufan@njust.edu.cn) or [wufanjlg@163.com](mailto:wufanjlg@163.com) (F. Wu)*

*c. National University of Defense Technology, Xi'an, 710106, P. R. China.*

*d. Department of Materials Science, Fudan University, Shanghai, 200433, PR China. E-mail: [Guangxingu@fudan.edu.com.cn](mailto:Guangxingu@fudan.edu.com.cn) (X. Guang).*

In Fig. S1a-c, different magnification TEM images of Fe<sub>3</sub>O<sub>4</sub> NPs were displayed. It is visible that Fe<sub>3</sub>O<sub>4</sub> NPs possess a relatively uniform spherical in shape with the diameters distribution in the range of 250-300 nm. The high magnification TEM image (Fig. S1c) demonstrates that the rough surfaces of Fe<sub>3</sub>O<sub>4</sub> NPs are caused by the formation of lots of small primary nanocrystals. Fig. S1d shows that the morphology of the pristine CuS reveals a flower-like structure with the diameter about 3 μm, and these the flower-like structured pristine CuS composed of thin nanoflakes disorderly with the average thickness of about 10 nm. This unique structure endows the CuS with the specific surface area and it is noticed that interspace between the nanoflakes can be a suitable position for generating bond with the Fe<sub>3</sub>O<sub>4</sub> NPs.

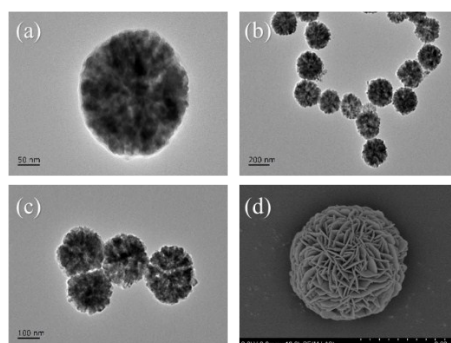


**Fig. S1** Different magnification TEM images of Fe<sub>3</sub>O<sub>4</sub> NPs (a - c) and SEM image of pristine CuS (d).

The EA properties of the composites is also determined by the loss tangent of electricity ( $\tan\delta_e = \varepsilon''/\varepsilon'$ ) and magnetism ( $\tan\delta_\mu = \mu''/\mu'$ ). The loss tangent can be calculated based on the data in Fig. 7, and the results are shown in Fig. S3. We extract the following observations: The frequency dependence of the  $\tan\delta_\mu$  exhibits very similar variation trend, while the  $\tan\delta_e$  of 40 wt% CSF filler loading displays a larger value than the other two samples. In this regard, the dielectric loss rather than the magnetic loss

contributes mainly to the EA of this sample.

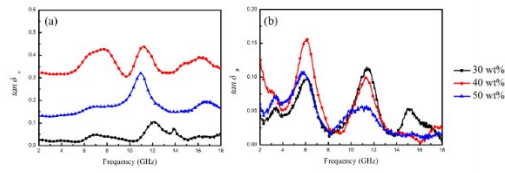


**Fig. S2** Frequency dependence of the dielectric loss tangent (a) and magnetic loss tangent (b) of CSF-160 heterostructure with the filler loading of 30 wt%, 40 wt% and 50 wt%.

Table 1†, we summarized the EA performances of some other CuS-based materials which have been published in recent years. The above results indicate that the as-prepared popcorn chicken-like CSF displays the strongest absorption properties and a broader absorption bandwidth with a thin absorber thickness (1.5mm).

**Table 1†** EA performance of typical CuS based composites reported in this work and recent literatures (PVDF: polyvinylidene fluoride)

Filler	Matrix	Optimal RL (dB)	Efficient EA bandwidth (GHz)	Thickness (mm)	Ref.
CSF-160	Wax	-61.32	4.15	1.50	This work
RGO/CuS	PVDF	-32.70	3.40	2.50	4
CuS	Wax	-17.50	3.00	1.10	5
CuS/ZnS	Wax	-22.60	2.20	3.00	6
Cu <sub>7.2</sub> S <sub>4</sub>	Wax	-36.60	6.00	1.60	7
CuS	Wax	-31.50	3.60	1.80	8

## References

- [1] Y. Liu, L. Yu, Y. Hu, C. Guo, F. Zhang, X. Wen. Lou, A magnetically separable photocatalyst based on nest-like  $\gamma$ -Fe<sub>2</sub>O<sub>3</sub>/ZnO double-shelled hollow structures with enhanced photocatalytic activity. *Nanoscale*. 4 (2012) 183-187.
- [2] M. Kim, H. Hafez, X. Chai, L. Besteiro, L. Tan, T. Ozaki, A. Govorov, R. Izquierdo, D. Ma, Covellite CuS nanocrystals: realizing rapid microwave-assisted synthesis in air and unravelling the disappearance of their plasmon resonance after coupling with carbon nanotubes. *Nanoscale*. 8 (2016) 12946-12957.
- [3] L. Cai, Y. Sun, W. Li, W. Zhang, X. Liu, D. Ding, N. Xu, CuS hierarchical hollow microcubes with improved visible-light photocatalytic performance. *RSC Adv*. 5 (2015) 98136-98143.
- [4] X. Zhang, G. Wang, Y. Wei, L. Guo and M. Cao, Polymer-composite with high dielectric constant and enhanced absorption properties based on graphene-CuS nanocomposites and polyvinylidene fluoride. *J. Mater. Chem. A*. 1 (2013) 12115-12122.
- [5] B. Zhao, X. Guo, Y. Zhou, T. Su, C. Ma, R. Zhang, Constructing hierarchical hollow CuS microspheres via a galvanic replacement reaction and their use as wide-band microwave absorbers. *CrystEngComm*, 19 (2017) 2178-2186.
- [6] X. Guan, P. Qu, X. Guan, G. Wang, Hydrothermal synthesis of hierarchical CuS/ZnS nanocomposites and their photocatalytic and microwave absorption properties. *RSC Adv*. 4 (2014) 15579-15585.
- [7] B. Zhao, G. Shao, B. Fan, W. Zhao, Y. Xie, R. Zhang, Synthesis of flower-like CuS hollow microspheres based on nanoflakes self-assembly and their microwave

absorption properties. *J. Mater. Chem. A*. 3 (2015) 10345-10352.

[8] M. Liu, G. Lv, G. Chen, Y. Qin, P. Sun, K. Zhou, X. Xing, C. He, Synthesis of Cu and Ni chalcogenides and evaluation of their properties for electromagnetic wave absorption. *RSC Adv.* 6 (2016) 102472-102481.